Accepted Manuscript

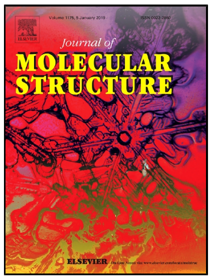

New poly(o-phenylenediamine)/modified-clay nanocomposites: A study on spectral, thermal, morphological and electrochemical characteristics

I. Khelifa, A. Belmokhtar, R. Berenguer, A. Benyoucef, E. Morallon

PII:	S0022-2860(18)31249-3
DOI:	10.1016/j.molstruc.2018.10.054
Reference:	MOLSTR 25783
To appear in:	*Journal of Molecular Structure*
Received Date:	23 August 2018
Accepted Date:	17 October 2018

Please cite this article as: I. Khelifa, A. Belmokhtar, R. Berenguer, A. Benyoucef, E. Morallon, New poly(o-phenylenediamine)/modified-clay nanocomposites: A study on spectral, thermal, morphological and electrochemical characteristics, *Journal of Molecular Structure* (2018), doi: 10.1016/j.molstruc.2018.10.054

New poly(o-phenylenediamine)/modified-clay nanocomposites: A study on spectral, thermal, morphological and electrochemical characteristics

I. Khelifa [1], A. Belmokhtar [1], R. Berenguer [2], A. Benyoucef [1,3] *, E. Morallon [2]

[1]*Laboratoire de Matériaux Application et Environnement, Université de Mustapha Stambouli Mascara, BP 763 Mascara 29000 (Algeria)*

[2]*Departamento de Química Física e Instituto Universitario de Materiales, Universidad de Alicante, Apartado 99, 03080 Alicante, Spain*

[3]*Laboratoire de Génie des Procédés et Chimie des Solutions, Université de Mustapha Stambouli Mascara. Bp 763 Mascara 29000 (Algeria)*

*Corresponding author

e-mail : abdelghani@ua.es

a.benyoucel@univ-mascara.dz

Telf.: (+213)771707184

Fax: (+213)45930118

Abstract

This work describes the synthesis and characterization of new poly(o-phenylenediamine) (PoPD)/modified-clay nanocomposite materials. For the synthesis, the raw clay (named as Mag) used in this study was from Maghnia (west Algeria), (Mag) clay was ion-exchanged with cobalt(II) sulfate hydrate and copper sulfate. The modified-clays were then dispersed in a oPD monomer-containing acidic solution to carry out in-situ intercalative oxidative polymerization by ammonium persulfate. XRF and XRD characterization reveal the success of ion-exchange to form highly intercalated Mag-Co and Mag-Cu clays. After polymerization, the disappearance of the interlayer-spacing diffraction peak for the PoPD-Mag-Cu and PoPD-Mag-Co nanocomposites points out fully exfoliation of the clay structure. The formation of intercalated PoPD into modified-clay nanocomposites was confirmed by XRD, TEM, TG analysis, FTIR spectroscopy and UV-vis studies. The nanocomposites show optical properties and the redox processes observed by cyclic voltammetry indicate that the reported polymerization into modified-clays leads to electroactive hybrid materials. All these properties make these polymer/clay nanocomposites attractive materials for multiple applications.

Keywords: Conjugated polymer; poly(orthophenylenediamine); Modifed-clay, Electrochemical properties.

1. Introduction

Conducting polymers generally show highly reversible redox behavior with a noticeable chemical memory and, hence, they have been considered as prominent new materials for the fabrication of sensors, organic batteries, diodes, electrocatalysts [1-3]. The properties of these materials strongly depend on the doping level, protonation level, size of ion dopant, and water content. Among a wide variety of conducting polymers, polyaniline (PANI) is one of the most attractive, and can be easily synthesized, without any special equipment or precautions, either by the electrochemical or the chemical oxidative polymerization methods. Moreover, the properties of this polymer can be further enhanced by derivation and hybridization with other materials.

Poly (p-phenylenedi-amine) (PpPDA) is an electroactive polymer of the aromatic diamines family. PoPD with a novel structure has stimulated increasing interest because of its variable conductivity, strong electroactivity, good optical and magnetic activity, and high environmental and thermal stability [4], which could extend the applications of the conducting polymers. This polymer is usually prepared by electrochemical polymerization [5, 6] with an irregular morphology as compared to that obtained by the chemical polymerization method [7, 8].

Inorganic-organic hybrid materials have become a field of intensive interest due to their multifaceted properties [9, 10]. These materials have given manifold high-tech applications on electrorheological fluids, anti-corrosion materials, molecular wires, sensor devices, smart windows, electrochemical devices, etc [11]. Layered phyllosilicates, such as smectite clays, stand out as the most commonly used materials to get PANI/Clay nanocomposites, being montmorillonite the most popular one because of its small particle size, large surface area, cation exchange properties and swelling capability [12, 13] and also due to its low cost and natural abundance [14-16]. Intercalated and/or exfoliated nanocomposites can be prepared by intercalation polymerization depending on the monomer/clay ratio. In the past, PANI/Clay nanocomposites were synthesized by emulsion intercalation [17-19], electrochemical [20, 21], inverse emulsion polymerization [22], in situ intercalation [23-27], and mechanochemical intercalation method [28, 29]. A higher intercalation level of PANI inside the clay gallery was achieved when the clay was chemically modified by various organic molecules before the polymerization [30, 31]. Despite the potential interest on the hybridization of PoPD, there are few works reporting the preparation and properties of PoPD/Clay nanocomposites.

In this paper, a novel material has been synthetized by oPDT with modified-clay at room temperature. The PoPDT/modified-Clay were characterized by UV-vis, FTIR, DRX, TG and TEM studies; their electrochemical behavior were investigated by cyclic voltammetry

2. Experimental

2.1. Materials

The monomer ortho-phenylenediamine (oPD) ($C_6H_8N_2$) (CAS No. 95-54-5) (Aldrich) was distilled under vacuum prior to use. Ammonium persulfate (APS) [$(NH_4)_2S_2O_8$] (CAS No. 7727-54-0), N-methyl-2-pyrrolidone (NMP) (CAS No. 872-50-4), ammonia solution (NH_4OH) (CAS No. 7664-41-7), $CoSO_4$ (CAS No. 60459-08-7), NaCl (CAS No. 7647-14-5) and $CuSO_4$ (CAS No. 7758-99-8) were of analytical purity and used without further purification.

2.2. Preparation of Maghnite (Mag)

The clay was obtained from Maghnia west of Algeria (named as raw-Mag). The clay sample was washed with distilled water to remove impurities; the raw-Mag (20 g) was crushed for 20 min using a Prolabo ceramic balls grinder. The sample was treated with a 2 M NaCl solution under continuous stirring, and washed several times with bi-distilled water, to remove chloride [27]. The absence of chloride was confirmed using silver nitrate. Then, the solid (Mag) was recovered by centrifugation, washed with abundant water, and finally dried at 105 ºC to be stored in tightly stoppered glass bottles for later use. The Mag-Co was prepared by the addition of 5 mmol of the solid Cobalt(II) sulfate hydrate to 1 L of a 1 % (w/v) aqueous dispersion of Mag under stirring for 24h. The Mag-Co was separated by centrifugation. The sediment was washed three times with distilled water. By the same protocol we prepared the Mag-Cu, using copper sulfate instead. The chemical composition obtained by X-ray fluorescence spectroscopy (XRF) for the three different clays is included in Table 1. Careful investigation reveals that the three samples were composed essentially of SiO_2, Al_2O_3, Fe_2O_3 and to very limited extent of K_2O and MgO. Some other oxides were also present but in very negligible proportions. The CuO content of Mag-Cu (3.58 wt%) are higher than those of the Mag-Co, while for the CoO content, the values are higher in the Mag-Co sample.

2.3. Preparation of the hybrid nanocomposites

PoPD-Mag-Co and PoPD-Mag-Cu nanocomposites were prepared by in-situ polymerization of oPD 0.22mol in acidic (HCl) dispersions of the modified clays. Firstly, the Mag was dried at 110 ºC for 24 h to remove moisture. Next, 1.0g of Mag was added to a 1M HCl solution and sonicated for 30 min with the assistance of an ultrasound probe. Subsequently, the monomer was added, and the solution was sonicated for another 30 min to promote the replacement of inorganic ions by molecules of oPD between the sheets of the clay. Finally, a 1M HCl solution containing the oxidizing agent (APS) was added dropwise to the solution containing the monomer and the clay under constant stirring (the molar of APS to oPD was 1:1). The polymerization of oPD was carried out at ambient temperature for 24h. The nanocomposites obtained were filtered, washed with distilled water and finally dried in oven at 50 ºC for 24 h.

2.4. Physicochemical Characterization

The X-ray diffraction was performed at a wavelength of 1.549 Å, at 40 kV and 40 mA using a Bruker CCD-Apex equipment with a X-ray generator (Cu K_α and Ni filter). UV-Vis spectra were obtained with Hitachi U-3000 model spectrometer in the 200-800 nm. The PoPD was separated from the clay using NMP as solvent. A Fourier transform infrared (FT-IR) spectrum was recorded using a Bruker Alpha in transmission mode.

Table 1. Composition (wt%) of Mag, Mag-Co and Mag-Cu obtained from XRF.

Composition (wt%)	SiO_2	Al_2O_3	Fe_2O_3	CaO	MgO	Na_2O	K_2O	TiO_2	CoO	CuO	SO_3
Mag	76.70	18.03	0.71	0.28	0.80	0.21	0.77	0.15	0.00	0.00	0.34
Mag-Co	73.41	18.82	1.79	0.68	1.05	0.31	1.11	0.13	2.38	0.01	0.21
Mag-Cu	75.55	14.51	1.08	0.72	0.95	0.25	1.09	0.12	0.00	3.58	0.15

Table 2. Peak maximum and *d*-spacing of Mag, Mag-Co, Mag-Cu and nanocomposites

Samples	Peak maximum, 2θ max (º)	Basal spacing, $d_{(001)}$ (Å)
Mag	6.92	12.77
Mag-Co	4.09	21.59
Mag-Cu	4.86	18.16
PoPD-Mag-Co	//	Exfoliated
PoPD-Mag-Cu	//	Exfoliated

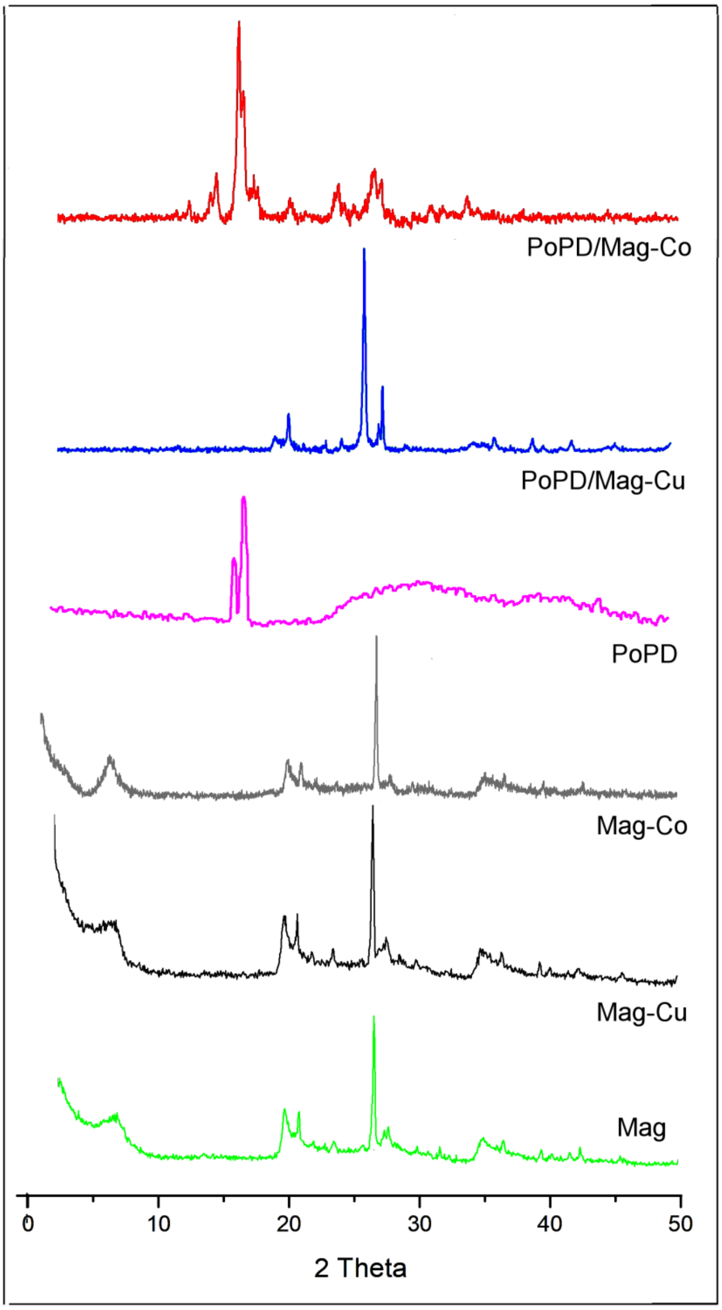

Fig. 1. XRD diffraction patterns of Mag, Mag-Co, Mag-Cu, PoPD, PoPD-Mag-Co and PoPD-Mag-Cu.

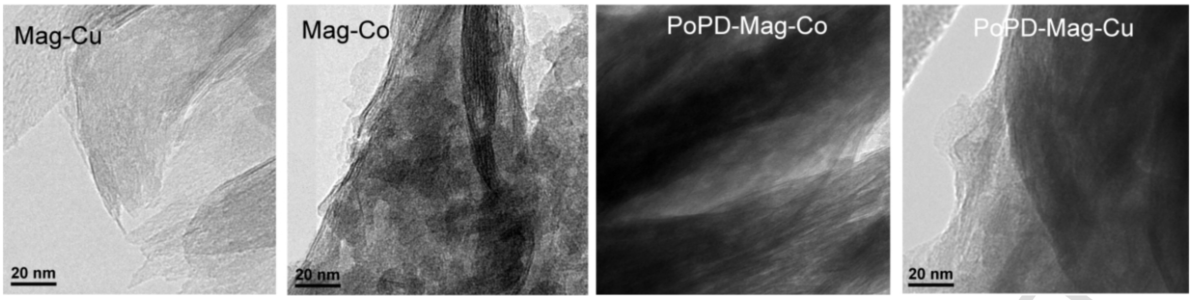

Fig. 2. TEM images of Mag-Cu, Mag-Co, PoPD-Mag-Co and PoPD-Mag-Cu.

Transmission Electron Microscopy (TEM) analyses were carried out using a JEOL microscope, model (JEM-2010) 200 kV. Thermogravimetric analyses (TGA) were conducted with a Du Pont thermogravimetric analyzer, with 10 mg samples from room temperature to 900 °C at a heating rate of 10 °C min^{-1} under a nitrogen atmosphere.

X-ray fluorescence spectroscopy of the powder clay was made using a Philips PW1480 equipment with a UNIQUANT II software to determine the elementary composition and the mass concentrations in elements. We use this method to analyze our samples.

2.5. Electrochemical characterization

The electrochemical characterization was performed using a conventional three-electrode electrochemical cell and a Bio-logic potentiostat/galvanostat SP-150. The electrolyte used was 1 M perchloric acid. The glassy carbon electrode (working electrode) was polished with BASi® polishing kit followed by washing with ultrapure water. A platinum wire was used as counter electrode and a reversible hydrogen electrode immersed in the same working electrolyte as reference electrode. The cyclic voltammetry was recorded at a scan rate of 50 $mV.s^{-1}$ using a potential range of -0.10 V at 1.00 V.

For the fabrication of working electrodes, the PoPD were first an amount of material is treated inN-methyl-2-pyrrolidone (NMP) as solvent [23]. Then, a drop of the resulting solution was placed on the glassy carbon electrode (0.07 cm^2 of geometrical area) and dried in air under an infrared lamp to remove the solvent.

3. Results and discussion

3.1. X-ray diffraction (XRD) studies

The XRD patterns of Mag, Mag-Cu, Mag-Co, PoPD-Mag-Cu and PoPD-Mag-Co are compared in Fig. 1. and in Table 2. The XRD patterns show that there was a shift of the 2θ angle of 6.92° for Mag (d_{001} = 12.77 Å) to 4.86° for Mag-Cu (d_{001} = 18.16 Å) and to 4.09° for Mag-Co (d_{001} = 21.59 Å) The shifting to smaller angles and, consequently, the increase in the basal spacing indicates the typical intercalation of the metal cation (cobalt or copper) in the clay [27]. The PoPD shows two sharp peaks at 16.47º and 17.38º individually, and a broad band centered at 25–36º, which reveal the polymer are partially crystallized [32]

In the PoPD-Mag-Cu and PoPD-Mag-Co nanocomposites, the characteristic peaks at low diffraction angles disappear, indicating the exfoliation of the clays. This result clearly reflects the formation of an intercalated polymer/clay nanocomposite. Furthermore, the diffraction peaks at 18º and 25º of Mag-Co remain in the pattern of PoPD-Mag-Co, but they became smaller and poorer. However, in the region between 13° and 21° five sharp crystalline peaks are observed at 14.06°, 14.52°, 16.25°, 16.61° and 17.36° that correspond to the periodicity d = 6.29, 6.09, 5.45, 5.33 and 5.10 nm. These peaks correspond to the crystal structure of PoPD [32, 33].

In the case of PoPD-Mag-Cu, the peak at 4.86º of Mag-Cu were disappeared, suggesting a high degree of exfoliation. Moreover, a group of the Mag-Cu characteristic diffraction peaks shifts to a higher angle at 19.12º, 20.07º, 22.90º, 25.86º and 27.21º indicating that there are obvious changes in the sample

3.2. Transmission Electron Microscopy (TEM)

The TEM was used to analyze the morphology of the nanocomposites and to confirm the X-ray diffraction results. Fig. 2. shows representative images obtained for Mag-Cu, Mag-Co, PoPD-Mag-Co and PoPD-Mag-Cu. Mag-Cu and Mag-Co present morphologies composed of Intercalated clay lamellae by cations (Cu^{+2} and Co^{+2}, respectively).

The dark zones observed in the images of PoPD-Mag-Cu and of PoPD-Mag-Co are attributed to PoPD matrix dispersed on the Clay surface. It is possible to observe that most of these PoPD are mainly concentrated at the Mag-Co surface compared with Mag-Cu, indicating a good compatibility between the inorganic and organic phases.

3.3. Fourier-transform infrared spectra (FTIR)

The FT-IR spectra of the four samples Mag-Co, Mag-Cu, PoPD-Mag-Co and PoPD-Mag-Cu are presented in Fig. 3. The spectra of the Mag-Cu and Mag-Co clays present three bands at 997-1000, 793-795 and 510-470 cm^{-1}. These features are attributed to the stretching vibration of Si−O bonds, the bending vibration of Al−OH bonds and the stretching vibration of Si−O−Al groups, respectively [34, 35]. All these features agree with the characteristic mineral structure of clays. The band at 3617-3626 cm^{-1} is assigned to the stretching mode of an inner hydroxyl group (In −OH), which are in the plane common to both the tetrahedral and octahedral sheets and this band which is typical of the stretching of the internal −OH groups in the kaolinite structure, Their movement is restricted as a result of chemical bonding between the silica and alumina sheets. Usually, this internal hydroxyl group is not significantly affected by inter lamellar modifications, and do not participate to the establishment of hydrogen bonds with the inserted molecules [36, 37].

Apart from these clay-characteristic features, the spectrum of the PoPD-Mag-Co nanocomposite showed additional bands. The broad one centered at around 3393 cm^{-1} can be associated to the N–H stretching vibration of secondary amine group in the PoPD chain. The bands at 1617 and 1524 cm^{-1} are assigned to the C=N and C=C stretching vibrations in quinoid and benzenoid rings, respectively. The small band at about 1366 cm^{-1} may be an indication of the imine C–N stretching vibration. Finally, the band at 801 cm^{-1} can be attributed to the out-of-plane bending vibration of benzene ring [38]. On the other hand, for the PoPD-Mag-Cu nanocomposite the N–H stretching is observed at 3244 cm^{-1}, the C=N stretching in quinoid ring at 1626 cm^{-1} and the C=C stretching in benzenoid ring at 1540 cm^{-1} and the band value Si–O of modified-clay shifted to higher value (997 cm^{-1}) by formacing the nanocomposites.

3.4. UV-Vis spectroscopy

The Fig. 4. shows the UV-vis absorption spectra of PoPD-Mag-Co and PoPD-Mag-Cu. In both cases, the absorption bands observed at 256 nm are assigned to the π-π* transition in aromatic heterocycles. These bands appeared also in the spectrum of the precursor (figure not shown). On the other hand, the bands at 408 nm suggest the existence of quinoid imine units (–C=N–) [39-41]. From this spectroscopic analysis, it can be concluded that the synthesized PoPD with modified-clay (Mag-Cu and Mag-Co) has a head-to-tail type arrangement with the benzenoid and quinoid structures in the phenazine-like backbone [40-42]. No differences in the synthesized polymer are observed with the two clays.

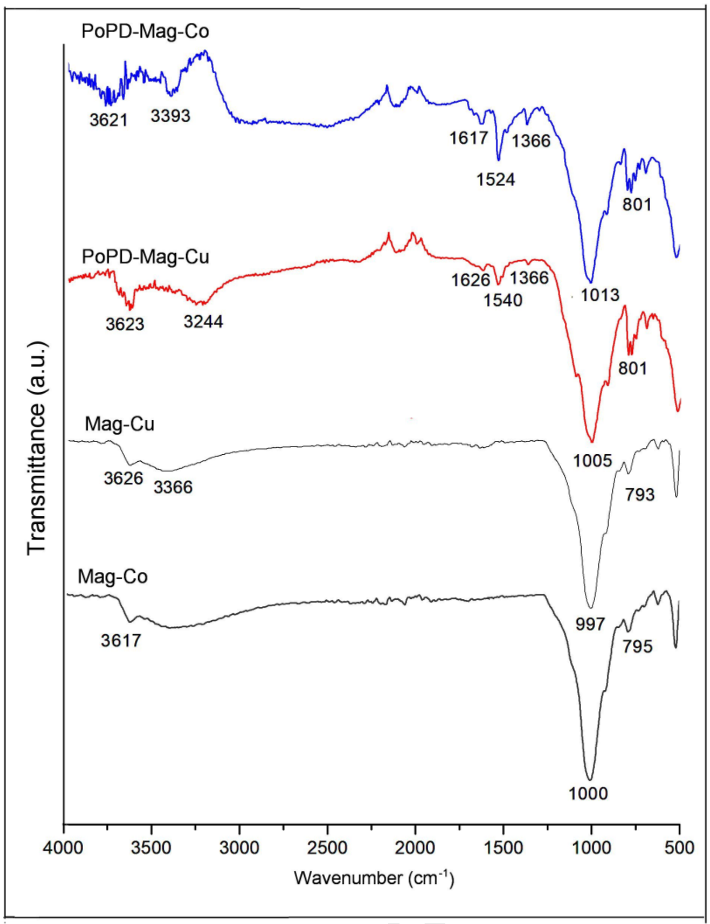

Fig. 3. IR absorption spectra of Mag-Co, Mag-Cu, PoPD-Mag-Co and PoPD-Mag-Cu.

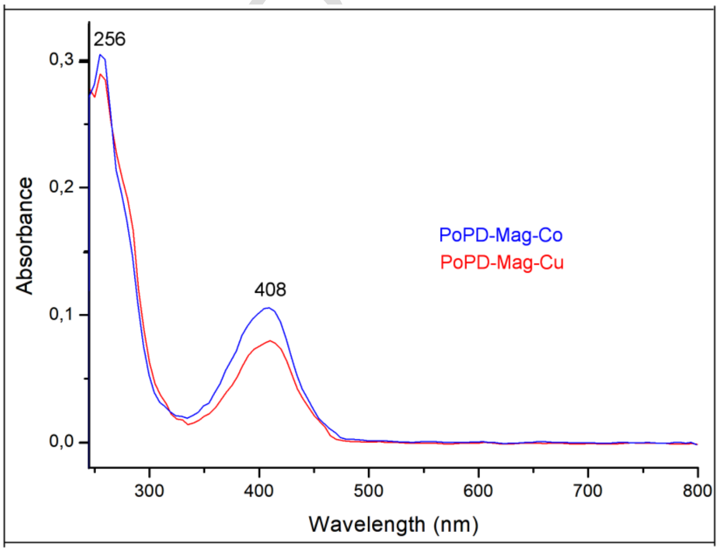

Fig. 4. UV-vis spectra of PoPD-Mag-Co and PoPD-Mag-Cu nanocomposites.

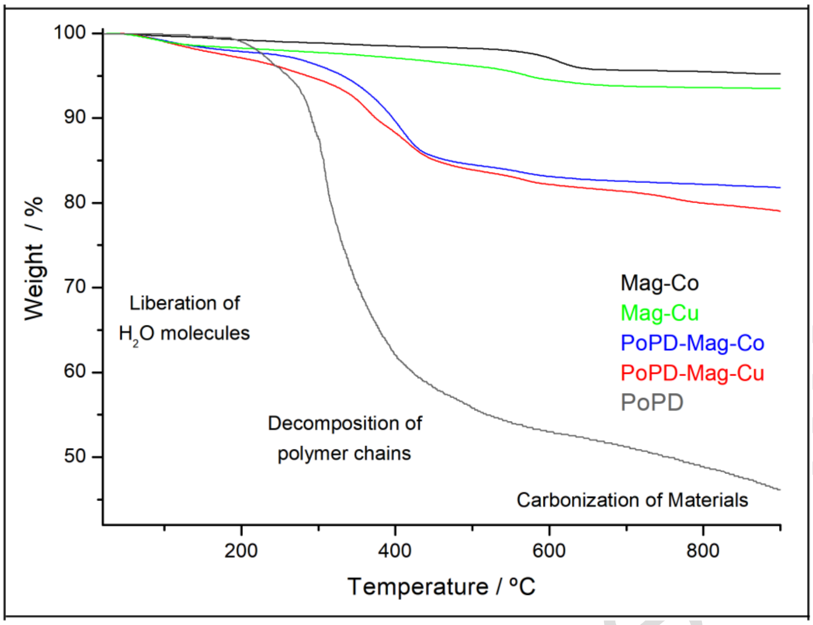

Fig. 5. TGA of Mag-Co, Mag-Cu, PoPD, PoPD-Mag-Co and PoPD-Mag-Cu obtained in nitrogen atmosphere at heating rate of 10°C/min.

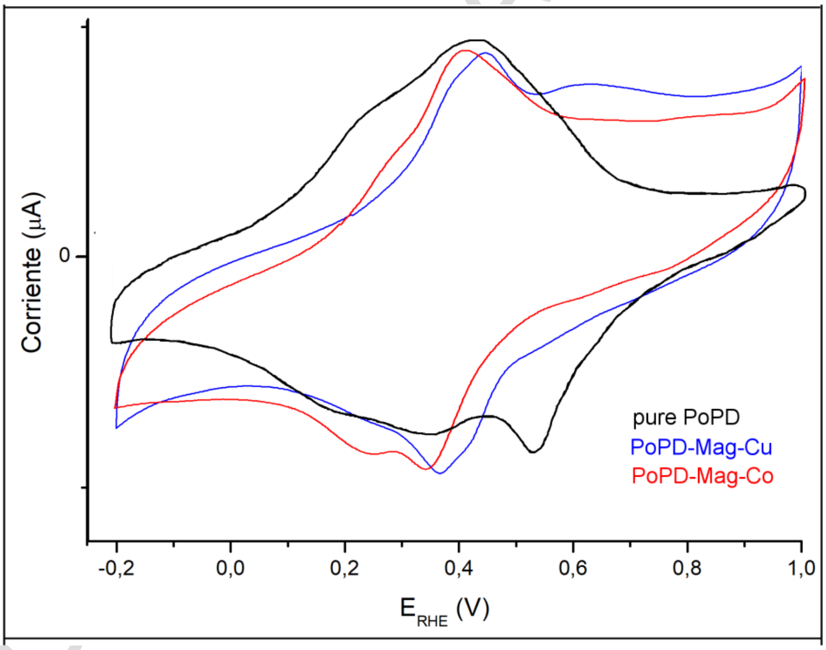

Fig. 6. Cyclic voltammograms recorded for a graphite carbon electrode covered by pure PoPD, PoPD-Mag-Co and PoPD-Mag-Cu in 1 M $HClO_4$ solution. Scan rate 100 mV.s^{-1}.

3.5. Thermal stability characteristics

Fig. 5. shows the thermogravimetric curves (TGA) plots of Mag-Cu, Mag-Co, PoPD-Mag-Cu and PoPD-Mag-Co. The TGA curves of Mag-Cu and Mag-Co presents a weight loss in the temperature range of 25 ºC to 220 ºC, which can be assigned to the removal of the physically adsorbed water located in the sheets [23-27]. In the following temperature range, the weight loss refers to the removal of the coordinated water and the structural water released from the clay framework [24-26]. For PoPD curve then shows stability up to 220°C, this sample displayed an accelerated weight loss at 250-600 °C due to the pyrolysis of the polymer, similar to the previously reported results [32]. The two nanocomposites thermogram shows that the decomposition of PoPD backbone chains is initiated at 440 ºC. Therefore, the content of PoPD in the PoPD-Mag-Cu and PoPD-Mag-Co nanocomposites can be calculated to be 11.09 % and 13.14 %, respectively. It can be inferred that the content of PoPD in the PoPD-Mag-Co is higher than in the case of PoPD-Mag-Cu nanocomposite, which is also consistent with the results of XRD.

3.5. Electrochemical properties

Fig. 6. shows the voltammograms of the different nanocomposites and the PoPD polymer. The pure polymer shows two main oxidation peaks at 210 mV and 400 mV in the forward scan; however, three distinguish cathodic peaks are observed in the reverse scan indicating that three redox processes are produced in the polymer [41, 43]. Fig. 5 shows the voltammogram of the PoPD-Mag-Co which is similar to that of pure PoPD; however, only two redox processes are presented. In addition, the main difference between these two materials is the shifting of the potential redox processes which in the case of PoPD-Mag-Co appear to more negative values. In the case of PoPD-Mag-Cu nanocomposite, the voltammetric profile shows

the first main redox process at 443/366 mV and the shoulder at lower potentials. Moreover, a clear oxidation peak is observed at higher potential values (around 608 mV). These differences in electrochemical behaviour are thought to be due only to the structural differences in the PoPD systems, the PoPD obtained by in-situ polymerization of monomers within the interlayer of Mag-Co and Mag-Cu are electroactives

4. Conclusions

In conclusion, it was shown that PoPD/modified-clay nanocomposites can be synthesized via in situ oxidative polymerization methods. Structural and physico-chemical characterizations by using various techniques have revealed that the Mag clays can be ion-exchanged to incorporate Co and Cu, first, and can be exfoliated during polymerization by triggering PoPD chain growth within the modified-clay sheets. Apart from optical properties, the good electrochemical response and the observed redox processes indicate that the polymerization into modified-clay produces electroactive polymer/clay nanocomposites with great potential for multiple applications.

Acknowledgements

The authors wish to acknowledge the directorate General of Scientific Research and Technological Development (DGRSDT) Algeria. Ministerio de Economía y Competitividad and FEDER is acknowledged for financial support (MAT2016-76595-R).

References

[1] U. Olgun, M. Gulfen. Synthesis of fluorescence poly(phenylenethiazolo[5,4-d]thiazole) copolymer dye: Spectroscopy, cyclic voltammetry and thermal analysis. Dyes Pigments 102 (2014) 189-195.

[2] M.S. Freund, B.A. Deore, Self-doped Conducting Polymers, John Wiley & Sons. (2007).

[3] U. Olgun, M. Gülfen. Doping of poly(o-phenylenediamine): Spectroscopy, voltammetry, conductivity and band gap energy. Reactive & Functional Polymers. 77 (2014) 23-29

[4] T. Siva, K. Kamaraj, S. Sathiyanarayanana, Electrosynthesis of poly(aniline-co-o-phenylenediamine) film on steel and its corrosion protection performance. Progress in Organic Coatings. 77 (2014) 1807-1815

[5] M. Abdelsalam. S.S. Al-Juaid, A.H. Qusti. A.A. Hermas. Electrochemical deposition of a carbon nanotube-poly(o-phenylenediamine) composite on a stainless steel surface. Synthetic Metals. 161 (2011) 153-157.

[6] J.L.O. Martínez. B.I.F. Mancilla. A.V. Rios. E.A.Z. Contreras. Poly(ortho-phenylenediamine-co-aniline) based copolymer with improved capacitance. Journal of Power Sources. 366 (2017) 233-240

[7] J. Stejskal, Polymers of phenylenediamines, Prog. Polym. Sci. 41 (2015) 1-31.

[8] X. Wang, P. Liu, Improving the electrochemical performance of polyaniline electrode for supercapacitor by chemical oxidative copolymerization with p-phenylenediamine. J. Ind. Eng. Chem. 20 (2014) 1324-1331.

[9] P.G. Romero. Hybrid Organic-Inorganic Materials. In Search of Synergic Activity. Advanced Materials. 13 (2001) 163-174

[10] N. Srivastava, Y. Singh, R.A. Singh. Preparation of intercalated polyaniline/clay nanocomposite and its exfoliation exhibiting dendritic structure. Bull. Mater. Sci. 34 (2011) 635-638.

[11] T.J. Pinnavai, G.W. Beall. Polymer-clay nanocomposites (New York: Wiley) (2001).

[12] G.M. Do Nascimento, V.R.L. Constantino, R. Landers, M.L.A. Temperini. Spectroscopic characterization of polyaniline formed in the presence of montmorillonite clay. Polymer. 47 (2006) 6131-6139.

[13] Q.Y. Soundararajah, B.S.B. Karunaratne, R.M.G. Rajapakse, Montmorillonite polyaniline nanocomposites: preparation, characterization and investigation of mechanical properties, Mater. Chem. Phys. 113 (2009) 850-855.

[14] P. Bober, J. Stejskal, M. Špírková, M. Trchová, M. Varga, J. Prokeš, Conducting polyaniline-montmorillonite composites. Synthetic Metals. 160 (2010) 2596-2604,

[15] Y. Zhang, Y. Shao, T. Zhang, G. Meng, F. Wang, High corrosion protection of a polyaniline/organophilic montmorillonite coating for magnesium alloys, Prog. Org. Coat. 76 (2013) 804-811.

[16] C.M. De León-Almazan , I.A.E. Moreno. U.P. García, J.L.R. Armenta. Polyaniline/clay nanocomposites. A comparative approach on the doping acid and the clay spacing technique. Synthetic Metals. 236 (2018) 61-67.

[17] B.H. Kim, J.H. Jung, S.H. Hong, J. Joo, A.J. Epstein, K. Mizoguchi, J.W. Kim, H.J. Choi. Nanocomposite of polyaniline and Na^+-montmorillonite clay. Macromolecules. 35 (2002) 1419-1423.

[18] B.H. Kim, J.H. Jung, S.H. Hong, J.W. Kim, H.J. Choi, J. Joo. Physical characterization of emulsion intercalated polyaniline-clay nanocomposite. Current Applied Physics. 1 (2001) 112-115

[19] D.H. Song, H.M. Lee, K.H. Lee, H.J. Choi. Intercalated Conducting Polyaniline-clay Nanocomposites and their Electrical Characteristics. Choi. J. Phys. Chem. Solid. 69 (2008) 1383-1385

[20] K.C. Chang, G.W. Jang, C.W. Peng, C.Y. Lin, J.C. Shieh, J.M. Yeh, J.C. Yang, W.T. Li. Comparatively electrochemical studies at different operational temperatures for the effect of nanoclay platelets on the anticorrosion efficiency of DBSA-doped polyaniline/Na+-MMT clay nanocomposite coatings. Electrochim Acta. 52 (2007) 5191-5200

[21] G.M. Nascimento, A.C.M. Padilha, V.R.L. Constantino, M.L.A. Temperini. Oxidation of anilinium ions intercalated in montmorillonite clay by electrochemical route. Colloids and Surfaces A: Physicochemical and Engineering Aspects. 318 (2008) 245-253

[22] R. Ullah, S. Bilal, A.A. Shah, K. Ali, F. Alakhras. Synthesis and characterization of polyaniline doped with polyvinyl alcohol by inverse emulsion polymerization. Synthetic Metals. 222 (2016) 162-169

[23] A. Belmokhtar, A. Benyoucef, A. Zehhaf, A. Yahiaoui, C. Quijada, E. Morallon. Studies on the conducting nanocomposite prepared by polymerization of 2-aminobenzoic acid

with aniline from aqueous solutions in montmorillonite. Synthetic Metals 162 (2012) 1864-1870.

[24] F. Chouli, A. Benyoucef, A. Yahiaoui, C. Quijada, E. Morallon. A conducting nanocomposite via intercalative polymerisation of 2-methylaniline with aniline in montmorillonite cation-exchanged. J Polym Res 19 (2012) 1-9.

[25] I. Toumi, A. Benyoucef, A. Yahiaoui, C. Quijada, E. Morallon. Effect of the intercalated cation-exchanged on the properties of nanocomposites prepared by 2-aminobenzene sulfonic acid with aniline and montmorillonite. Journal of Alloys and Compounds. 551 (2013) 212-218.

[26] A. Zehhaf, E. Morallon, A. Benyoucef. Polyaniline/montmorillonite nanocomposites obtained by in situ intercalation and oxidative polymerization in cationic modified-clay (sodium, copper and iron). Journal of Inorganic and Organometallic Polymers and Materials. 23 (2013) 1485-1491.

[27] M. Khaldi, A. Benyoucef, S. Bousalem, A. Yahiaoui, E. Morallon. Synthesis, Characterization and Conducting Properties of Nanocomposites of Successively Intercalated 2-Aminophenol with Aniline in modified-Montmorillonite. Journal of Inorganic and Organometallic Polymers and Materials. 24 (2014) 267-274.

[28] S. Yoshimoto, F. Ohashi, Y. Ohnishi, T. Nonami. Synthesis of polyaniline–montmorillonite nanocomposites by the mechanochemical intercalation method. Synthetic Metals. 145 (2004) 265-270

[29] I.B. Abbes, E. Srasra. Characterization and AC conductivity of polyaniline-montmorillonite nanocomposites synthesized by mechanical/chemical reaction. Reactive and Functional Polymers 70 (2010) 11-18

[30] K.H. Chen, S.M. Yang. Polyaniline-Montmorillonite Composite Synthesized by Electrochemical Method. Synthetic Metals. 135-136 (2003) 151-152

[31] W. Jia, E. Segal, D. Kornemandel, Y. Lamhot, M. Narkis, A. Siegmann. Polyaniline-DBSA/organophilic clay nanocomposites: synthesis and characterization. Synthetic Metals. 128 (2002) 115-120.

[32] Y.L. Min, T. Wang, Y.G. Zhang, Y.C. Chen. The synthesis of poly(p-phenylenediamine) microstructures without oxidant and their effective adsorption of lead ions. Journal of Materials Chemistry. 21 (2011) 6683-6689

[33] N.N. Binitha, S. Sugunan. Polyaniline/Pillared Montmorillonite Clay Composite Nanofibers. Journal of Applied Polymer Science. 107 (2008) 3367-3372.

[34] N. Salahuddin, M.M. Ayad, M. Ali, Synthesis and characterization of polyaniline–organoclay nanocomposites. Journal of Applied Polymer Science 107 (2008) 1981-1989.

[35] J.A. Marins, B.G. Soares. A facile and inexpensive method for the preparation of conducting polyaniline–clay composite nanofibers. Synthetic Metals 162 (2012) 2087-2094.

[36] R.L. Frost, J. Kristof, J.M. Schmidt, J.T. Kloprogge. Raman spectroscopy of potassium acetate-intercalated kaolinites at liquid nitrogen temperature. Spectrochim Acta A. 57 (2001) 603-609.

[37] K.B. Brandt, T.A. Elbokl, C. Detellier. Intercalation and interlamellar grafting of polyols in layered aluminosilicates. D-Sorbitol and adonitol derivatives of kaolinite. Journal of Materials Chemistry. 13 (2003) 2566-2572.

[38] G.C. Marjanović, M. Trchová, E.N. Konyushenko, P. Holler, J. Stejskal. Chemical Oxidative Polymerization of Aminodiphenylamines. J. Phys. Chem. B, 112 (2008) 6976-6987.

[39] S. Daikh, F.Z. Zeggai, A. Bellil, A. Benyoucef. Chemical polymerization, characterization and electrochemical studies of PANI/ZnO doped with hydrochloric acid and/or zinc chloride: Differences between the synthesized nanocomposites. Journal of Physics and Chemistry of Solids. 121 (2018) 78-84

[40] S. Benyakhou, A. Belmokhtar, A. Zehhaf, A. Benyoucef. Development of novel hybrid materials based on poly(2-Aminophenyl disulfide)/Silica Gel : preparation, characterization and electrochemical studies. Journal of Molecular Structure 1150 (2017) 580-585.

[41] A. Bekhoukh, A. Zehhaf, A. Benyoucef, S. Bousalem, M. Belbachir. Nanoparticules Mass Effect of ZnO on the Properties of Poly(4-Chloroaniline)/Zinc Oxide Nanocomposites. Journal of Inorganic and Organometallic Polymers and Materials. 27 (2017) 13-20.

[42] F. Chouli, I. Radja, E. Morallon, A. Benyoucef. A Novel Conducting Nanocomposite Obtained by p-Anisidine and Aniline With Titanium(IV) Oxide Nanoparticles: Synthesis, Characterization, and Electrochemical Properties. Polymer Composites. 38 (2017) 254-260.

[43] S.A. Gharaibeh, E.N.E.H. Molero, V.I. Birss. Electrochemical and Mass Change Study of the Growth of Poly-(o-Phenylenediamine) Films on Au Substrates. Journal of The Electrochemical Society. 160 (2013) 344-354.

Highlights

1- A simple and facile method was used to synthesize prepared a PoPD/Modified-clay

2- The presence of PoPD in intercalated modified-clay (by Cu^{+2} and Co^{+2}) is observed in all nanocomposites.

3- Characterizations confirm the presence of PoPD with modified-clay.

4- The nanocomposites is more thermal stability than the PoPD

5- Good electrochemical response has been observed for all samples.